Cavallaro, A.; Solis Díaz, C.; Garcia, PR.; Ballesteros, B.; Serra Alfaro, JM.; Santiso, J. (2012). Epitaxial Films of the proton-conducting Ca-doped LaNbO4 material and study of their charge transport properties. Solid State Ionics. 216:25-30. doi:10.1016/j.ssi.2012.03.033.

Epitaxial films of the proton-conducting Ca-doped LaNbO4 material and a study of their charge transport properties

Article *in* Solid State Ionics · May 2012

DOI: 10.1016/j.ssi.2012.03.033

CITATIONS
2

READS
77

6 authors, including:

A. Cavallaro
Imperial College London
34 PUBLICATIONS **386** CITATIONS
SEE PROFILE

Cecilia Solís
Technische Universität München
42 PUBLICATIONS **604** CITATIONS
SEE PROFILE

Jose Manuel Serra
Universitat Politècnica de València
173 PUBLICATIONS **3,103** CITATIONS
SEE PROFILE

Epitaxial Films of the proton-conducting Ca-doped $LaNbO_4$ material and study of their charge transport properties

Andrea Cavallaro[1*], Cecilia Solis[2], Pablo Garcia[1],Belen Ballesteros[1], Jose M. Serra[2] and José Santiso[1]

[1] Research Centre for Nanoscience and Nanotechnology, CIN2 (CSIC-ICN) Campus UAB. Bellaterra, Barcelona. Spain.

[2] Instituto Tecnología Química, ITQ (CSIC-UPV) Campus UPV. Valencia. Spain

*Corresponding author. Tel: +34 935813724

E-mail address: acavallaro@cin2.es (A.Cavallaro)

Solid State Ionics 216 (2012) 25–30

Abstract

Ca-doped $LaNbO_4$ (LCNO) material has shown outstanding stability in harsh environments in combination with moderate proton-conductivity in polycrystalline samples at intermediate temperatures below 800ºC under wet atmosphere. However, in polycrystalline materials the role of grain boundaries is believed to play a predominant role in protonic conductivity, which may make more difficult the study of the intrinsic properties of the material. For that reason the present study focuses on the preparation of epitaxial films by pulsed laser deposition on single crystal substrates like $NdGaO_3$ (110). Under certain deposition conditions the films grow epitaxially with monoclinic structure (fergusonite) and *b*-axis orientation. A polymorph change between monoclinic and tetragonal structure has been observed at 250ºC. The film charge transport properties are analyzed under different atmospheres, dry and wet O_2 and H_2 as well as under deuterated conditions by using D_2 and D_2O in order to check for the characteristic isotopic effect of the proton transport. Although a certain proton conductivity was observed under reducing wet atmosphere unexpected large DC conductivity values (of

about 5.5 S/cm for the 80 nm thin LCNO film at 800ºC in dry O_2) have been observed for all films and ambient conditions.

Keywords : $LaNbO_4$, Proton conductor, Epitaxial thin film, Pulsed Laser Deposition.

1.1 Introduction

Among proton conducting materials, the acceptor-doped rare-earth ortho-niobates represent a good compromise between transport properties and material chemical stability. As shown by Haugsrud *et al.* [1,2] in this class of material protonic, ionic and electronic conduction may coexist, depending on the ambient conditions. In particular below 800 ºC in wet atmospheres protons are clearly the predominant carriers in polycrystalline. Despite the modest conductivity values reported for lanthanum niobates, this essentially pure proton conductor can be used as electrolyte in proton conducting fuel cell (PCDC) devices upon reducing its thickness down to micrometer scale (thus reducing the diffusion length for proton transport) [3,4]. One of the most promising candidates within this family is $La_{1-x}Ca_xNbO_{4-\delta}$ with a proton conductivity of 10^{-3} Scm^{-1} at 800 ºC in wet atmosphere (x=0.005-0.01) [1]. Polycrystalline films of about 2 μm thickness of 0.5% Ca-substituted $LaNbO_4$ compound have been deposited by PLD with ASR values of 0.4 $\Omega \cdot cm^2$ at 600 °C comparable to expected bulk values [5]. Several studies have been recently performed in order to increase the transport properties by other doping strategies [6,7]. On the other hand grain boundary resistivity of this kind of compounds has been reported to be higher than grain interior resistivity [8] and thus an important parameter to be taken into account. Structural studies performed on bulk $LaNbO_4$ ortho-niobate materials indicate that they can exist in two polymorphs [9,10]: i) the low-temperature *fergusonite* phase crystallized in the monoclinic-crystal system (space group $I2/c$); and ii) a high-temperature tetragonal phase, isostructural with the tetragonal *scheelite* structure (space group $I4_1/a$). The phase transformation in $LaNbO_4$ bulk material occurs at a temperature in the range of 490 ºC to 525 ºC. A recent report [11] shows that the growth of grain-boundary-free yttrium-doped barium zirconate films resulted in the achievement of the largest proton conductivity ever reported for ceramic proton conductors. The present work focuses on the deposition and characterization of first epitaxial thin films of $La_{0.995}Ca_{0.005}NbO_{4-\delta}$

(LCNO) in order to study the intrinsic properties of the material minimizing the grain boundary contributions.

To analyze the transport properties of LCNO material it is necessary to understand the defect equilibrium under different atmosphere conditions. Defect equilibrium reactions are summarized in Table 1 [1,6]. In undoped $LaNbO_4$ material the generation of oxygen vacancies is mainly due to the oxygen exchange with atmosphere, as it is depicted in the equilibrium Equation (1) while intrinsic electron-hole pair formation by thermal excitation over the band gap follows Equation (2). As it has been previously studied the oxygen vacancy concentration might be increased by partial substitution of La^{+3} for divalent dopants [12]. Equation (3) describes the compensation of the introduced negative defects (Ca'_{La})) through the formation of oxygen vacancies ($V_O^{\cdot\cdot}$). It has also to be considered that protons are incorporated in the oxide structure through oxide hydration following Equation (4) which implies the water dissociation into OH^- or H^+ which accommodates in an oxygen vacancy and lattice respectively. The electroneutrality condition can be written as in equation (5) by assuming the charge compensation of doping defects for oxygen vacancies and protons, as well as for electronic carriers, where brackets denote concentrations.

Table 1: Main defect equilibrium reactions

$O_O^x + 2h^\bullet \Leftrightarrow \frac{1}{2}O_2(g) + V_O^{\bullet\bullet};\quad K_{Ox} = \left[O_O^x\right]\left[V_O^{\bullet\bullet}\right]^{-1}\cdot p^2\cdot pO_2^{-1/2}$	(1)
$0 \Leftrightarrow e^{/} + h^\bullet;\quad K_e = n\cdot p$	(2)
$2CaO + Nb_2O_5 \Leftrightarrow 2Ca_{La}^{/} + 2Nb_{Nb}^x + V_O^{\bullet\bullet} + 7O_O^x;\quad K_{Ca'_{La}} = [Ca_{La}^{/}]^2\cdot[Nb_{Nb}^x]^2\cdot\left[V_O^{\bullet\bullet}\right]$	(3)
$H_2O(g) + V_O^{\bullet\bullet} + O_O^x \Leftrightarrow 2OH_O^\bullet;\quad K_{hydr} = [OH_O^\bullet]^2\cdot pH_2O^{-1}\cdot[V_O^{\bullet\bullet}]^{-1}$	(4)
$2[V_O^{\bullet\bullet}] + [OH_O^\bullet] + p = [Ca_{La}^{/}] + n$	(5)

Electronic conduction (*p*- and *n*- type) and ionic (oxygen and protonic) transport contribute to the total conductivity of the material and the final contribution of each partial conductivity will depend on their corresponding carrier concentration and mobility.

In dry oxidizing conditions protons and electrons are negligible ($[OH_O^\bullet] \to 0$ and $n \to 0$ in equation (5)). For very strongly oxidizing conditions *p*-type electronic conductivity is

proportional to the introduced negative defects ($[Ca'_{La}]$). At high and intermediate pO_2, from equation (1), the *p*-type electronic conductivity has a pO_2 power dependency of +1/4, as observed for common operating conditions, e.g. 800-1000 ºC and pO_2=1-10^{-4} atm [1,7]. At lower pO_2 electronic carrier concentration is substantially reduced compared to oxygen vacancy concentration and ionic conductivity may prevail. Therefore total conductivity is independent of the pO_2 and equals to 1/2 of the introduced negative defects ($[Ca'_{La}]$).

2. Experimental

Ca-doped $LaNbO_4$ thin films were obtained by using Pulsed Laser Deposition (PLD) technique. A dense pellet was prepared from 0.5% Ca-doped $LaNbO_4$ commercial powder (Cerpotech) by uniaxial pressing at 72 MPa and sintering at 1300 ºC for 5 h. The densified $La_{1-x}Ca_xNbO_{4-\delta}$ bulk material was used as target for the PLD process. The films were grown by using a Compex Pro 201 KrF excimer laser (λ=248 nm) at 1 Hz pulse repetition rate at a laser fluence in the range of 1-3 J/cm^2. The target to substrate distance has been maintained constant, *d*=53 mm. Deposition temperature and oxygen partial pressure have been varied between 500 ºC and 900 ºC and $4.3\cdot10^{-2}$ – $6.7\cdot10^{-2}$ mbar respectively. The LCNO film thickness has been varied in the range of 20-80 nm by adjusting the number of laser pulses. Single crystals of (110)-oriented $NdGaO_3$ (NGO, from CrysTec GmbH) have been used as substrates for the epitaxial thin film growth. This substrate cut has been chosen for its good match with the LCNO crystal cell, (mismatch of about +0.3% between average cell parameter $\bar{a}_{NGO}$=5.456 Å of $(110)_{NGO}$ plane and $\bar{a}_{LCNO}$=5.437 Å of $(010)_{LCNO}$ plane calculated from reported cell parameters a_{LCNO}=5.633 Å, c_{LCNO}=5.261 Å and β=94.15º, of monoclinic *I*2/*c* structure [9]), as well as for its low electrical conductivity compared with typical $SrTiO_3$ or $LaAlO_3$ single crystals. This last requirement is essential in order to reduce the substrate contribution (generally the substrates are 0.5 mm thick) to the total thin film electrical response and to characterise the weak conductance of very thin ionic conducting films, particularly in the in-plane configuration. Reflection high energy electron diffraction (RHEED) was used in-situ during the PLD film deposition in order to monitor the crystal quality of the growing film (R-DEC 30KV e-gun at incidence angle <1º). AFM topography analysis (tapping mode, 5100 SPM, Agilent Technologies) was also

performed on the as-deposited samples in order to analyse surface roughness. X-ray diffraction analysis was carried out by performing 2theta/omega scans along with reciprocal space mapping (RSM) in a Panalytical X'Pert diffractometer with CuKa radiation. X-ray reflectometry (XRR) was used for film thickness determination. DC conductivity measurements were carried out by standard two-point technique, by painting two parallel Ag electrodes and attaching corresponding Ag wires. A constant current ramp (from -20 up to 20 μA, each 4.5 μA) was supplied by a programmable current source (Keithley 2601) while the voltage drop was detected by a multimeter (Keithley 3706). The total conductivity was analyzed as a function of oxygen partial pressure and in moist atmospheres (by using 2.5% of H_2O and D_2O) in the temperature range from 400 ºC up to 800 ºC. The different pO_2 were reached by using calibrated gas mixtures (O_2-Ar) provided by Linde. Measurements in reducing atmospheres have been performed in dry or wet 5% H_2 and 5% D_2 in Ar by using 0.025 atm of H_2O and D_2O respectively when necessary.

Sample cross-sections for HRTEM observation were prepared using focused ion beam (FIB) on a Zeiss Crossbeam 1560 XB microscope. A 4 nm thick coating of Au and 16 nm of Pt was evaporated onto the sample before FIB milling to protect the region of interest and prevent charging. Coarse milling was done at 30 kV and then samples were thinned to approximately 50 nm thickness at 2 kV. Samples were examined in a scanning transmission electron microscope JEOL JEM 2100, equipped with EDX, and STEM detectors.

3. Results and discussion

In order to find the optimum conditions for pulsed laser deposition of LCNO thin films on $NdGaO_3$ (110)-oriented single crystal substrates, some preliminary experiments were carried out varying oxygen partial pressure, laser fluence, substrate temperature and number of laser pulses. Fig.1 presents the XRD analysis of an 80 nm LCNO thin film. The only presence of (0*k*0) film reflections along with substrate reflections indicate that LCNO grows with its long *b*-axis out of plane. No trace of any other orientation was detected.

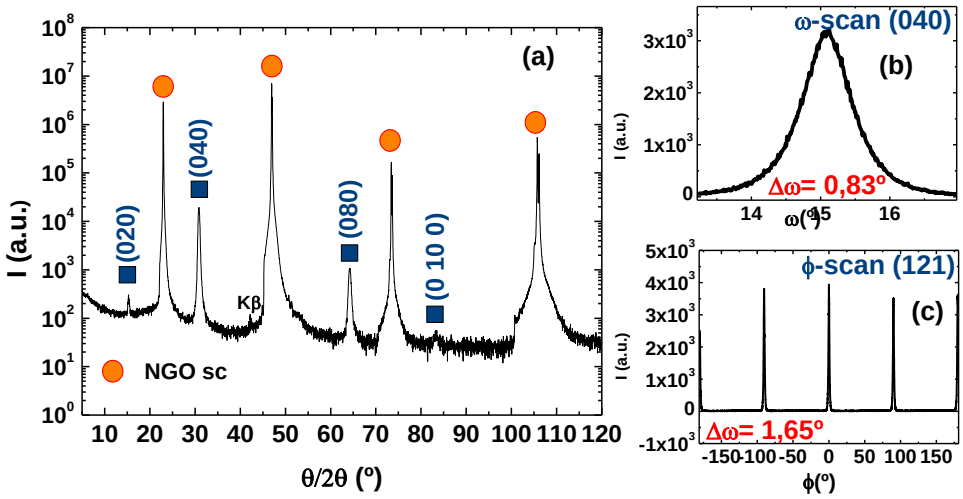

Fig. 1: θ/2θ-scan of an 80 nm LCNO thin film grown on NdGaO3 (110) single crystal (a). The ω-scan analysis of the LCNO (040) reflection and the ϕ-scan analysis of the LCNO (121) reflection are respectively (b) and (c).

Rocking curve (ω-scan) analysis of symmetric (040) LCNO reflection along with ϕ-scan of asymmetric (121) LCNO reflection reveal that the thin films are both out–of-plane and in-plane textured. The reflection positions confirm the following epitaxial relation between film and substrate: LCNO (010)//NdGaO3(110) and LCNO [101]// NdGaO3 [001]. Fully epitaxial *b*-axis oriented LCNO thin films were obtained in a wide range of deposition conditions. Substrate temperature of 900 ºC, pO_2= 4.3 10^{-2} mbar, and laser fluence of 3 J/cm^2 have been chosen as the optimal PLD deposition conditions.

Table 2 summarizes FWHM values of ω and ϕ–scans for LCNO samples with different thickness (27, 44, 80 nm) deposited at the same optimized PLD conditions. In plane and out-of-plane parameter analysis reveal a lower FWHM for the thinnest film (27 nm), which indicates a better degree of epitaxial growth. Thicker samples show larger FWHM values for both ω and ϕ scans. As expected, an increasing film thickness induces the appearance of slightly misoriented domains when reducing the influence of the epitaxial single crystal orientation. However, the spread in ϕ angle may also arise from the mosaicity of monoclinic microdomains oriented in different in-plane directions.

Table 2: FWHM values measured in ω and ϕ scan for a 27, 44 and 80 nm LCNO thin films. The *a* and *b* LCNO cell parameters calculated by RSM have been also included.

Thickness (nm)	Δω	Δϕ	*a* (Å)	*b* (Å)
27	0.28º	1.27º	5.394	11.594
44	0.87º	1.69º	5.378	11.629
80	0.83º	1.65º	5.399	11.592

Fig. 2 shows the XRD reciprocal space map of an asymmetric (1 10 1) LCNO reflection for a 27 nm thin film along with (332) $NdGaO_3$ substrate reflection. From this type of maps it is possible to directly extract average out-of-plane and in-plane parameters of the film (*b*-and *a*-axis parameters, respectively for the relative film-substrate orientation). The *b* and *a* parameters of the LCNO films (included in Table 2) are very close to those expected for bulk material, average in-plane $\bar{a}_{LCNO}$=5.437 Å and out-of-plane b_{LCNO}=11.666 Å (calculated from reported monoclinic structure *a*=5.633, *b*=11.666 and *c*=5.261 Å, β=94.15º at 21ºC [9]) and point out that the LCNO film is already completely relaxed after the 27 nm film thickness.

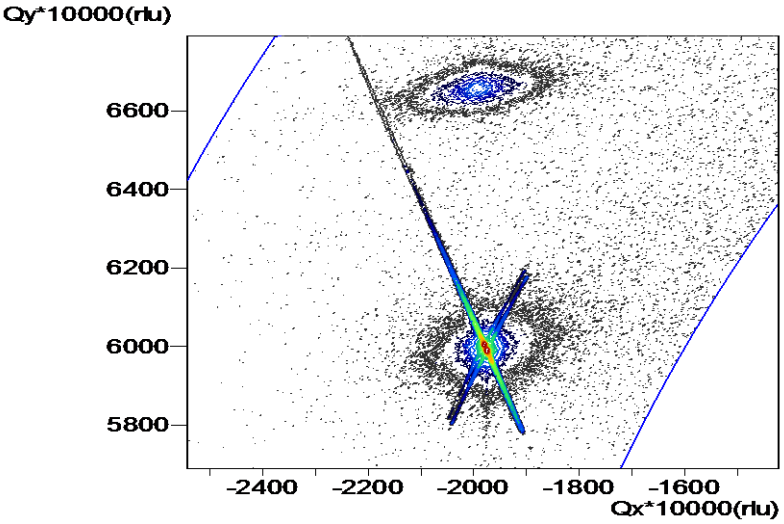

Fig. 2: Reciprocal space map of a 27 nm LCNO thin film deposited on NGO (110) oriented single crystal in the region of the 1 10 1 LCNO and 332 NGO indicates the epitaxial arrangement of the layer.

RHEED in-situ analysis (zone axes [110]) correlated with the surface AFM analysis of the three samples is presented in Fig.3. The electron diffraction patterns already visible at the very early stages of the film growth shows overlapping of 3D (spots) and 2D

(streaks) patterns, indicative of a non-perfectly flat epitaxial growth mode, also confirmed by the granular surface morphology of the three LCNO films observed by AFM. While the film surface roughness is increasing with the film thickness, from a RMS of 0.83 nm to the 1.67 nm of the thickest one, the connection between grains seems to improve. The RHEED pattern of the thickest film shows narrower strikes with less contribution of the 3D (spotty) pattern, which corroborates the presence of a denser surface. The spot patterns and distances measured by RHEED are consistent with the epitaxial arrangement observed by XRD.

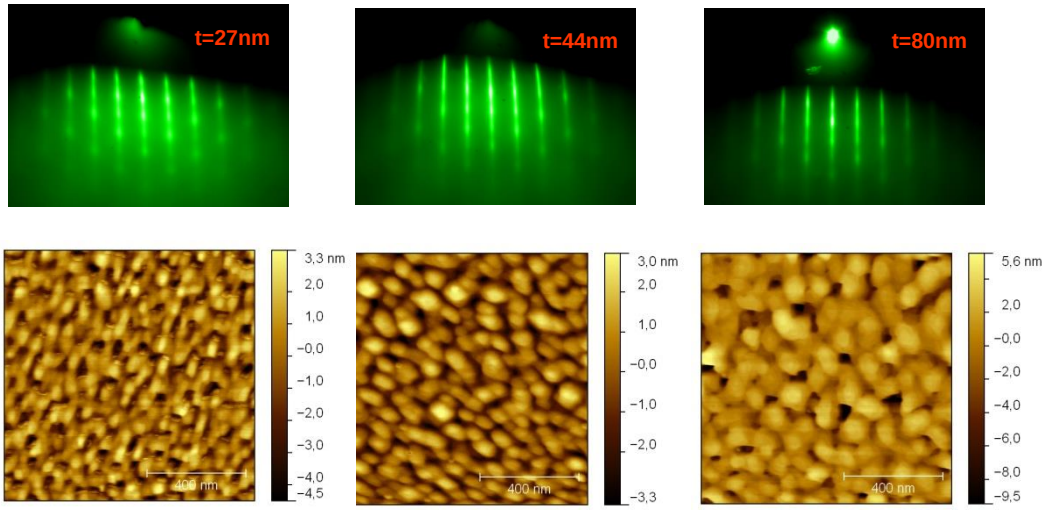

Fig. 3: On top, in situ RHEED (Reflection High Energy Electron Diffraction) of three samples after the LCNO deposition process (27, 44 and 80 nm thin films); on the bottom, AFM analysis of the same three sample surfaces with increasing thickness (from left to right).

Figure 4 shows the TEM analysis of LCNO(80 nm)/NGO(110) film cross-section. The low magnification image shows vertical lines that correspond to low angle grain boundaries, typical of a columnar PLD's growth, clearly visible across the film thickness (4a) from substrate interface up to the surface. The film appears dense and homogeneous and the HRTEM analysis of the top part of the LCNO film (4b) shows a good crystalline quality. The region close to the substrate up to a thickness of about 30-40 nm shows a different contrast that may indicate the formation of a different microstructure. However, XRD analysis of the thinnest film (27 nm) still reveals a dominant contribution of epitaxial *b*-axis oriented LCNO material. The contrast could be related to the coexistence of a secondary phase, but no evidences have been obtained neither by TEM or XRD analysis. Fast Fourier Transform (FFT) analysis presented in

the inset of the same HRTEM image shows the presence of the major interplanar distances: A= 0.57 nm; B= 0.22 nm; and C= 0.31 nm. The appearance of 020 planes (corresponding to A) indicate unequivocally the presence of monoclinic structure as it was shown in simulations (by CaRine) of the reciprocal space for monoclinic and tetragonal LCNO structures in the same zone-axis as HREM image.

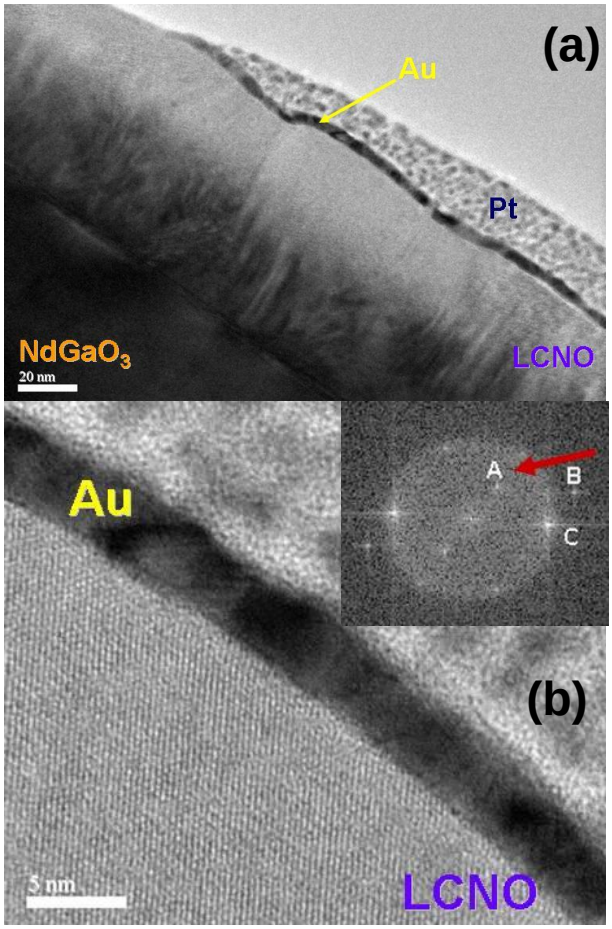

Fig. 4: (a) TEM lamella of an 80 nm LCNO film on NGO(110) substrate. On top of the LCNO film a gold and platinum layers have been deposited during the lamella's preparation. (b) HREM cross section of the top part of the thin film and in (c) the Fourier Transform Analysis of the same HREM image are presented.

In order to find additional evidences supporting the observation of monoclinic LCNO structure at room temperature we analysed the film thermal expansion coefficient by XRD. The *b*-axis cell parameter of 80 nm thick film grown at the optimized PLD conditions has been measured (from the angular position of 040 reflections) at different temperatures in the range from 50 to 600 ºC, with a heating chamber (Anton Paar DHS-1100C) under static air. No damage, neither delamination nor crack formation, were observed in the thin films after heat treatment. Results are shown in Fig.5. Two regions

with a clear different slope have been observed, being the calculated thermal expansion coefficients α of 16.6 10^{-6} $^{o}C^{-1}$ below 250 ^{o}C, and 7.67 10^{-6} $^{o}C^{-1}$ above this temperature. These values are consistent with reported expansion coefficients $15 \cdot 10^{-6}$ $^{o}C^{-1}$ and $8.6 \cdot 10^{-6}$ $^{o}C^{-1}$ for bulk monoclinic and tetragonal structures, respectively [13]. This suggests a phase transformation from monoclinic to tetragonal structure near 250 ^{o}C. This temperature is much lower than the one found for bulk LCNO material (500 ^{o}C). Variations in phase transition temperature in epitaxial films have been frequently observed in a wide variety of perovskite-related oxides [14] and are generally associated to subtle film structure variations and domain formation induced by the substrate matching. In this particular case this reduction is very likely related to the as-deposited structure of LCNO film crystal domains, which probably present reduced monoclinic distortion than bulk material. Certainly film growth at deposition temperatures, well above phase transition temperature, will stabilise tetragonal structure. However, during the cooling down process, it is very likely that LCNO matching with the rectangular plane of (110) NGO substrate will provide enough energy for hindering, to a certain extent, the monoclinic in-plane shear strain increases (β angle increase), along with the *a* and *c* axis difference, corresponding to LCNO transformation to equilibrium monoclinic structure. Still, shear strain may be partially released, within the explored film thickness range, showing a tendency towards the formation of incipient monoclinic domains at room temperature (as it has been observed by TEM, but not by XRD), but it is sufficient to drop down the phase transition temperature (at least for the measured thickness of 80 nm).

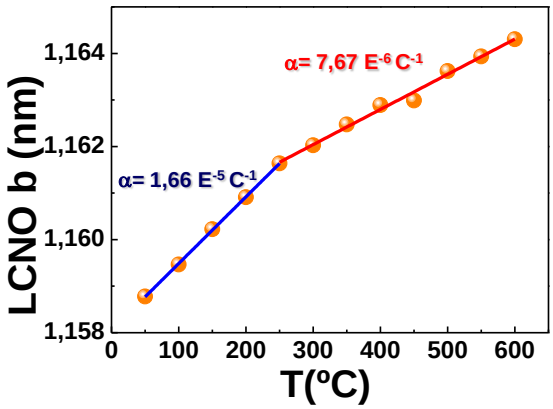

Fig. 5: XRD high-temperature analysis of an LCNO80 nm/NGO(110)SC sample. The 2θ value of the (040) LCNO symmetric reflection with the heating temperature has been plotted in the graph.

Concerning charge transport characterisation of the films, Fig. 6 shows the total in-plane conductivity measured in dry and wet (H_2O and D_2O) oxygen atmosphere for the three samples (27, 44 and 80 nm). One of the most remarkable observation is that the conductivity of these films is about 5-20 S/cm (800 ºC in dry O_2), 3-4 orders of magnitude higher than the one measured for the bulk polycrystalline material [1] ($8 \cdot 10^{-4}$ S/cm at the same 800 ºC in dry O_2 conditions). The enhanced values of the total conductivity (oxygen ionic and *p*-type electronic conductivity for LCNO in dry O_2) might be expected for epitaxial films due to the low density of grain boundaries, which may have a substantial blocking effect in bulk material, as well as favorable transport properties along a particular crystallographic orientation in case of anisotropic materials. Specifically, grain boundaries in Sr doped $LaNbO_4$ present up to 4 orders of magnitude higher resistivity than grain interior in wet atmospheres [8]. However, the total conductivity showed in these films is still orders of magnitude higher than that observed in bulk samples and it is not plausible that only grain boundary effects are responsible for this huge increase in conductivity.

Interface strain effects can favor both electronic or ionic conductivity, as it has been proved previously in other epitaxial thin films of mixed ionic-electronic and protonic conducting oxides [11,12,15,]. Alternatively, this huge increase of the total conductivity might be attributed to the appearance of a highly conducting secondary phase. Although, the combination of both XRD or TEM analysis rules out the presence of a major secondary phase, the main reason for the increase in the conductivity as well as its nature, either electronic or ionic, remains unclear. The conductivity results shown in Fig. 6 suggest that there is no substantial hydration effect (conductivity in dry and wet atmospheres are almost equal) irrespective of the LCNO film thickness, which indicates the absence of measurable protonic transport in oxidizing environments. Moreover, the high conductivity values are probably related to the fast electronic transport, which also prevails in wet atmospheres. Fig. 7 presents the conductivity at 700 °C and 400 °C as a function of the pO_2 (*log-log* scale) for the 80 nm thick film. For both temperatures there is a linear dependency with pO_2 with positive slopes slightly below +1/4. Power dependence with positive exponent close to ¼ in oxidizing conditions is characteristic

of a regime with predominant *p*-type electronic conductivity (as it was discussed previously in the introduction). This fact agrees with the predominant *p*-type electronic conductivity observed in oxidizing conditions for the polycrystalline bulk material [1] due to the higher mobility of electronic carriers than that of ionic species despite the low electronic carriers concentration.

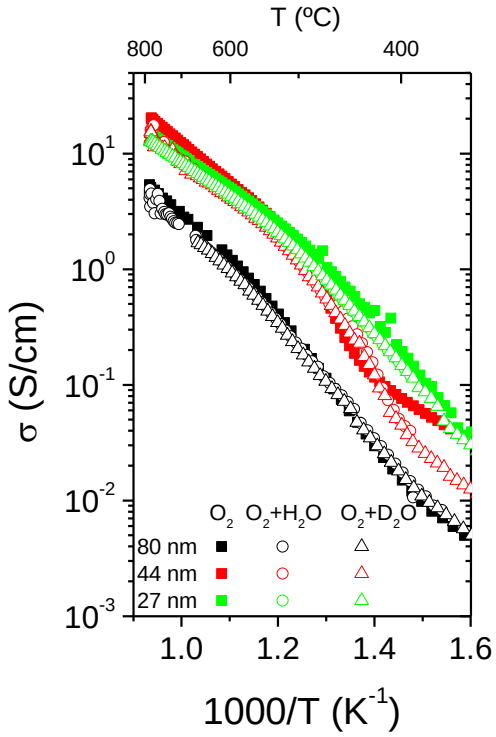

Fig. 6: Total conductivity of LCNO films of 80, 44 and 27 nm measured in dry and wet O_2 (where wet is either normal water or deuterated water).

On the other hand, from the conductivity measurements (Fig. 6), a change in the activation energy E_a can be observed. This change in the activation energy occurs at 350-450 ºC, a temperature a bit higher than that observed for the monoclinic to tetragonal phase transformation found at 250 ºC for the 80 nm epitaxial film, but lower than that observed for phase transition in bulk samples. E_a in the high temperature range (500-800 ºC) reaches values of 0.6 eV (0.8 eV for the 80 nm film) while at lower temperatures (300-400 ºC) E_a is around 0.75 eV. The transition temperature, between 350 and 500 ºC, where the conductivity changes the activation energy, has been reported to be a consequence of the mobility changes when monoclinic shear distortion β angle increases through the second order phase transition [1]. It can be appreciated that although conductivity of the 27 and 44 nm films are similar, the thickest shows lower conductivity. This higher conductivity in the thinnest films suggests again the

possibility of an additional interface contribution, not confirmed yet, since the contribution of this interfacial conductivity will increase with decreasing thicknesses. In order to avoid possible errors produced by any interface contributions further conductivity measurements were carried out on the 80 nm thick sample.

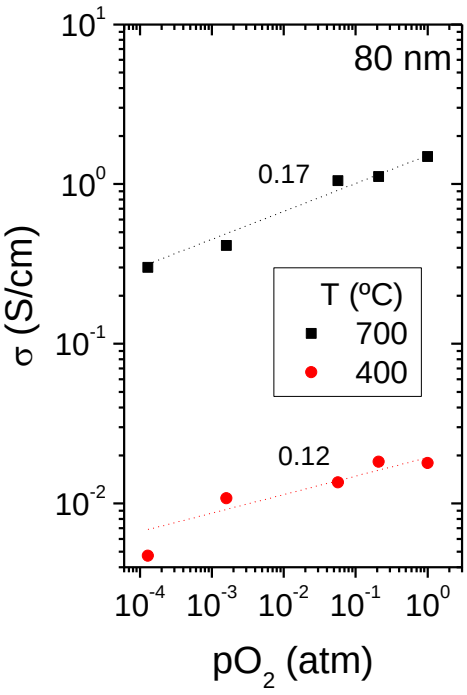

Fig. 7: Conductivity at 700 °C and at 400 °C in dry atmospheres as a function of pO_2 of an 80 nm thick film.

In figure 8 the total conductivity of the 80 nm LCNO thin film in dry and wet H_2 and D_2 is presented. The isotopic effect can be confirmed by a direct comparison between conductivity in H_2+H_2O (open circles) and D_2+D_2O (open triangles) that shows higher conductivity in wet H_2 than in wet D_2, slightly lower than the theoretical $\sqrt{2}$ value and confirming the protonic nature of this transport. In dry atmospheres measurements in H_2 and in D_2 are the same and similar to those obtained in D_2+D_2O. Calculated E_a values are 0.66 eV above 550 ºC and 0.81 eV below 450 ºC, values very similar to those reported for bulk material. As it was mentioned before it can also be appreciated an important increase in conductivity of the films compared to the reported values for polycrystalline bulk material in similar wet reducing atmospheres [2]. A similar increase in conductivity in epitaxial thin films, of around 2 orders of magnitude with respect the bulk material, has been also reported for the protonic conductor yttrium-doped barium zirconate (BZY) [11] and has been ascribed to the minimization of less-

conductive grain boundary regions in the high quality growth epitaxial thin films. Despite this huge increase in conductivity, LCNO epitaxial thin films conductivity in wet hydrogen is still significantly lower that reported values for BZY epitaxial films growth on MgO [11] (at 650 ºC LCNO presents 0.13 S/cm and BZY around 0.5 S/cm and at 450 ºC LCNO presents 0.0048 S/cm and BZY around 0.06 S/cm).

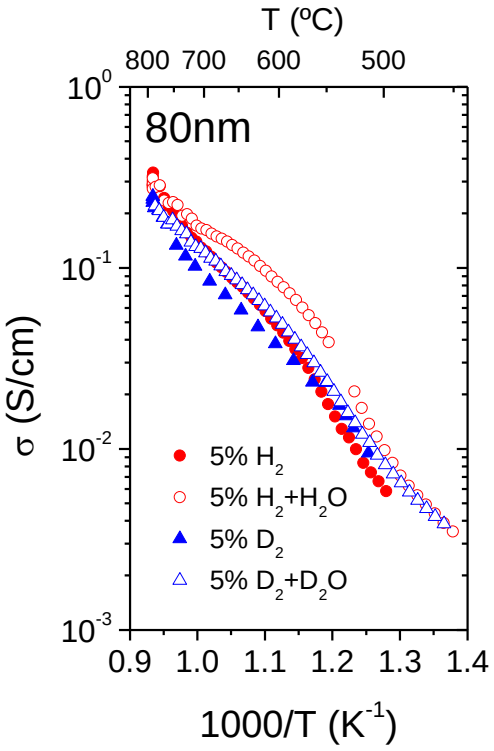

Fig. 8: Total conductivity of the LCNO80 nm film in 5% H2, 5% H_2+H_2O, 5% D_2 and 5% D_2+D_2O.

Total conductivity results in different atmospheres in this LCNO epitaxial thin film have shown a huge increase in the total conductivity ascribed principally to electronic transport in oxidizing conditions and both protonic and electronic transport in reducing atmospheres. This improvement in conductivity observed in these films is difficult to explain despite their epitaxial nature and their very low density of grain boundary area. This fact might indicate that microstructural differences between the epitaxial LCNO films and bulk material may considerably affect the protonic diffusion mechanism. The present research study consists of a preliminary step towards a more complete comprehension of the relationship between microstructure and protonic transport properties of LCNO material in the form of epitaxial films.

4. Summary and Conclusions

Experimental PLD deposition conditions have been optimized and epitaxial thin films of monoclinic 0.5% Ca-doped $LaNbO_4$ (LCNO) on NGO(110) single crystals have been obtained. Reciprocal space map (RSM) analyses of three samples with increasing thickness have shown full strain relaxation already for the thinnest film. Strain energy is probably released by the 3D growth mode of the LCNO film observed by the RHEED in situ and AFM analyses. The transition from monoclinic to tetragonal phase, typically observed at a temperature of 500 ºC for bulk LCNO, has been found to be of 250 ºC for an 80 nm LCNO thin film. We believe that a certain influence of the substrate, and particularly the lower mismatch of the tetragonal phase with respect to the monoclinic one is responsible for the observed reduction of the transition temperature by stabilizing the tetragonal LCNO phase at a lower temperature. The planar DC-conductivity of LCNO films has been measured under different atmospheres and temperatures. It shows 3 orders of magnitude higher conductivity in dry O_2 compared with the results obtained by Haugsrud *et al*. [1,2] for a bulk LCNO. This might be related to the absence of high angle grain boundaries (GB) characteristic of polycrystalline bulk ceramics. It is well known that these GB block part of the ionic conductivity of oxygen and particularly in proton conductors [11]. On the other side the higher conductivity for the thinnest film in all different atmosphere conditions suggests an additional interface contribution (which has not yet been confirmed). In reducing atmospheres there exists a 2 orders of magnitude increase in protonic conductivity, similar to that observed in BZY epitaxial films with respect to the bulk material [11] and ascribed to both the low density of conductivity limiting GB and some other chemical and/or structural change that influences protonic transport in the epitaxial films. Some basic questions remain still unclear, as for example the predominance of the *p*-electronic conductivity (not only under O_2 atmosphere, but even under more reducing conditions up to 10^{-4} atm) with respect to the predominant protonic one expected in wet Ar. Some further HRTEM investigations on the LCNO-NGOsc interface and of the LCNO low angle grain boundaries will be necessary for a full comprehension of the defect chemistry dominating in these epitaxial LCNO thin films. At the moment the film protonic conductivity was only confirmed under H_2 atmosphere by the isotopic effect.

Acknowledgment

The authors also acknowledge the financial support of European Union (FP7 Project EFFIPRO - Grant Agreement 227560), Spanish Government (MAT2008-04931, ENE2008-06302, Consolider-Ingenio 2010-CSD2008-023 CSIC Intramural 200880I093 grants). One author (A.C.) acknowledges the support of a "Juan de la Cierva" postdoctoral fellowship from the Spanish Ministry of Science and Innovation.

References

[1] R. Haugsrud, T. Norby, *Solid State Ionics* 177 (2006) 1129-1135
[2] R. Haugsrud and T. Norby *Nature Mater.* 5 (2006) 193-196.
[3] A. Magrasó, M.-L. Fontaine, Y. Larring, R. Bredesen, G. E. Syvertsen, H. L. Lein, T. Grande, M. Huse, R. Strandbakke, R. Haugsrud, T. Norby, *Fuel Cells* 11 (2011) 17-25.
[4] C. Solís, V. B. Vert, M. Fabuel, J. M. Serra, *J. Power Sources* 196 (2011) 9220-9227.
[5] A. Magrasó, H. Xuriguera, M. Varela, M. F. Sunding, R. Strandbakke, R. Haugsrud, and T. Norby. *J. Am. Ceram. Soc*., 93 (2010) 1874–1878 (2011)
[6] A. D. Brandao, J. Gracio, G.C. Mather, V. V. Kharton, D. P. Fagg 1984 (2011) 863-870.
[7] C. Solís and J. M. Serra, Solid State Ionics 190 (2011) 38-45.
[8] H. Fjeld, D.M. Kepaptsogplou, R. Haugsrud, T. Norby *Solid State Ionics* 181 (2010) 104-109.
[9] L. Jian and C.M. Wayman *J. Am. Ceram. Soc.*, 80 (1997) 803-806.
[10] F. Vollum, F. Nitsche, S.M Selbach and T. Grande *Acta Crystallographica A* 49 (1993) 595-600.
[11] D. Pergolesi, E. Fabbri, A. D'Epifanio, E. Di Bartolomeo, A. Tebano, S. Sanna, S. Licoccia, G. Balestrino, and E. Traversa, *Nature Mater*. 9, (2010) 846-852
[12] C. Solís, M.D. Rossell, G. Garcia, G.Van Tendeloo, J. Santiso, *Adv. Funct. Mater.* 18 (2008) 785-793.
[13] T. Mokkelbost, H. L.Lein, P.E.Vullum, R. Holmestad ,T.Grande, M.Einarsrud, *Ceramics International* 35 (2009) 2877–2883
[14] J. Cao and J. Wu, *Mater. Sci. Eng. R* 71 (2011) 35–52
[15] G. Garcia, M. Burriel, N. Bonanos, J. Santiso, *J. Electrochem. Soc.*,155 (2008) 28-32.